Effect of sine-Gaussian glitches on searches for binary coalescence

T Dal Canton[1], S Bhagwat[2], S V Dhurandhar[3] and A Lundgren[1]

[1] Albert-Einstein-Institut, Max-Planck-Institut für Gravitationsphysik, D-30167 Hannover, Germany

[2] Indian Institute of Science Education & Research, Central Tower, Sai Trinity Building, Pashan, Pune 411021, India

[3] Inter University Centre for Astronomy & Astrophysics, Ganeshkhind, Pune - 411 007, India

E-mail: tito.dalcanton@aei.mpg.de

Abstract. We investigate the effect of an important class of glitches occurring in the detector data on matched filter searches of gravitational waves from coalescing compact binaries in the advanced detector era. The glitches, which can be modeled as sine-Gaussians, can produce triggers with significant time delays and thus have important bearing on veto procedures as will be described in the paper. We provide approximated analytical estimates of the trigger SNR and time as a function of the parameters describing the sine-Gaussian (center time, center frequency and Q-factor) and the inspiral waveform (chirp mass). We validate our analytical predictions through simple numerical simulations, performed by filtering noiseless sine-Gaussians with the inspiral matched filter and recovering the time and value of the maximum of the resulting SNR time series. Although we identify regions of the parameter space in which each approximation no longer reproduces the numerical results, the approximations complement each other and together effectively cover the whole parameter space.

1. Introduction

Advanced interferometric gravitational-wave detectors are currently under construction and are expected to start delivering strain data in a few years. Major improvements over the first-generation interferometers will include a significantly better sensitivity curve at all frequencies of interest, which will effectively shift the sensitive band lower boundary from ~ 40 Hz to ~ 10 Hz [1, 2].

A promising source of gravitational-wave detections in the advanced interferometer era is represented by the inspiral and coalescence of compact binary systems (neutron star binaries, black hole-neutron star binaries and black hole binaries) [3]. The strain waveform associated with such events can be calculated to a good approximation at least for some regions of the parameter space describing the binary system [4]. Consequently, the classical data analysis pipeline for detecting such signals employs a filter matched

to the analytical waveform [5]. This approach consists in correlating the strain data with the waveform and producing an estimate of the signal to noise ratio (SNR) for that waveform. Triggers are then generated whenever the SNR exceeds a pre-defined threshold. Lists of triggers are independently produced for each detector and combined to obtain coincident triggers, which are then checked for consistency and passed on to more elaborate analysis. Similar search pipelines will be employed in the advanced detector era. However, in order to exploit the improved noise curves and extend the search to lower frequencies, the strain data will have to be filtered with significantly longer inspiral waveforms than used for past searches (up to tens of minutes as opposed to about one minute for BNS). In fact, the duration of the waveform in the interferometer output depends strongly on the low-frequency cutoff [6].

It is well known that first generation interferometers were affected by high rates of short-duration transients unrelated to astrophysical events and commonly known as *glitches*, most of which can be roughly modeled as short sine-Gaussian waveforms with a few cycles, i.e. a small Q-factor [7]. The typical effect of glitches on searches for binary coalescence was a significant deviation of the SNR distribution from what one would expect for perfectly Gaussian noise, i.e. a χ^2 distribution. Most glitches were ruled out as gravitational-wave candidates by monitoring *auxiliary channels* and their origin could rather be attributed either to the noisy environment of the detector (for instance seismic noise, weather, electromagnetic disturbances) or to unexpected behavior of the detector components (ADC saturation, problems with control systems and thermal compensation, scattered light) [8, 9]. Nevertheless, the surviving glitches affected the coincidence rate and thus weakened the ability to both confidently detect signals as well as set strong upper limits on the coalescence rate.

Unfortunately, despite the improved sensitivity, advanced detectors are expected to manifest similar glitches in their output, which will still pose significant challenges to future gravitational-wave searches. In particular, the longer BNS inspiral waveforms used to exploit the sensitivity at low frequency could lead to significant time delays between the occurrence of a glitch and the coalescence time of the resulting spurious trigger. Often, such delays will be much longer than the glitch duration and they will have to be taken into account when associating inspiral triggers with excitations of the auxiliary channels, or conversely, when using auxiliary channels to veto intervals of strain data.

For this reason, we investigate triggers generated by sine-Gaussian glitches interacting with a matched-filter search for inspiral gravitational waves in the advanced detector era. To this end we present approximations to the complex matched filter output and to the SNR time series, which is the quantity used for producing the inspiral triggers. We present three such approximations which complement each other and completely cover the parameter space of the sine-Gaussians, namely the central time t_0, the central frequency f_0 and the quality factor Q. We support the approximations with numerical simulations.

The paper is organized as follows. In section 2 we briefly review the matched

filter algorithm and fix the relevant notation. In section 3 we derive the approximated estimates for the SNR time series. In section 4 we compare these results to numerical simulations and we identify regimes where the different approximations are no longer acceptable. Section 5 discusses the implications of our results and possible ways to incorporate our estimations into veto procedures for the advanced era.

2. Matched filter

A matched filter search combines a detector strain data segment $s(t)$, the signal to be sought $h(t)$ and the one-sided power spectrum of the detector noise $S_{\rm n}(f)$ into a quantity representing the SNR as a function of the parameters describing the gravitational-wave source [6]. The SNR for a binary coalescing at time t is calculated as ‡

$$\rho(t) = \frac{|z(t)|}{\sigma} \tag{1}$$

where $z(t)$ is the output of the complex matched filter,

$$z(t) = 4\int_{f_{\rm L}}^{f_{\rm H}} \frac{\tilde{s}(f)\tilde{h}^*(f)}{S_{\rm n}(f)}{\rm d}f \tag{2}$$

and σ is the sensitivity of the detector to the sought after signal,

$$\sigma^2 = 4\int_{f_{\rm L}}^{f_{\rm H}} \frac{|\tilde{h}(f)|^2}{S_{\rm n}(f)}{\rm d}f. \tag{3}$$

In the above expressions, $\tilde{s}(f)$ is the Fourier transform of the pre-conditioned data segment and

$$\tilde{h}(f) = h_0 f^{-7/6} e^{-i\psi(f)} \tag{4}$$

is the inspiral signal template expressed in the frequency domain via the stationary phase approximation [10]. $f_{\rm L}$ and $f_{\rm H}$ are frequency cutoff values. Searches performed on first-generation detector data used $f_{\rm L} = 40$ Hz and for advanced interferometers $f_{\rm L} = 10$ Hz is expected. $f_{\rm H}$ is usually set to the frequency corresponding to the innermost stable circular orbit of a test mass orbiting a Schwarzschild black hole, i.e. $f_{\rm ISCO} = c^3/(6\sqrt{6}\pi GM)$.

Candidate inspiral triggers are identified as local maxima of the SNR crossing a pre-established threshold. Each trigger carries the set of associated parameter values, e.g. coalescence time and phase and binary component masses.

3. Response to a sine-Gaussian waveform

We are interested in calculating the response of the inspiral matched filter to a sine-Gaussian waveform, i.e. the SNR time series $\rho(t)$ after the center time of the sine-Gaussian. From $\rho(t)$ we want to estimate the maximum SNR $\hat{\rho}$ and the corresponding time $\hat{t}$.

‡ For simplicity and since search algorithms work with SNR time series, we only explicitly display the dependency on the coalescence time t and omit the other parameters.

The sine-Gaussian waveform can be written in the time domain as

$$s(t) = A \exp\left(-\frac{(t-t_0)^2}{\tau^2}\right) \cos(2\pi f_0 t + \phi_0) \tag{5}$$

where A is an overall amplitude, t_0 and f_0 are the location of the sine-Gaussian in time and frequency respectively, $\tau = Q/2\pi f_0$ is the time duration, Q is the dimensionless quality factor and ϕ_0 is the phase of the oscillation at $t = 0$. We are free to define the time origin as $t_0 = 0$, so that $\hat{t}$ represents the time delay between the sine-Gaussian and the inspiral trigger. Since the SNR is linear in the signal amplitude, we can also set $A = 1$. The sine-Gaussian can then be expressed in the frequency domain as

$$\tilde{s}(f) = \frac{\sqrt{\pi}}{2}\tau \exp\left(-\pi^2\tau^2(f-f_0)^2 + i\phi_0\right)\left[1 + \exp\left(-Q^2\frac{f}{f_0} - 2i\phi_0\right)\right]. \tag{6}$$

For $f_{\rm L} < f < f_{\rm H}$, the second exponential falls off very quickly as Q increases from 1, so we neglect it altogether. We can now also set $\phi_0 = 0$ since the SNR is not affected by global phase factors. Inserting (4) and the so-modified (6) into (2) we get

$$z(t) = 2\sqrt{\pi}\tau h_0 \int_{f_{\rm L}}^{f_{\rm H}} \frac{f^{-7/6}}{S_{\rm n}(f)} \exp\left(-\pi^2\tau^2(f-f_0)^2 + i\psi(f)\right) {\rm d}f. \tag{7}$$

In order to get an explicit expression, we approximate $\psi(f)$ with the simple *Newtonian chirp* [11]

$$\psi(f) = 2\pi f t - 2\phi - \frac{\pi}{4} + \frac{3}{128}(\zeta f)^{-5/3} \tag{8}$$

where t is the coalescence time, ϕ is the orbital phase at coalescence, $\zeta = \pi G\mathcal{M}/c^3$ and $\mathcal{M} = (m_1 m_2)^{3/5}/(m_1+m_2)^{1/5}$ is the chirp mass of the binary system composed of masses m_1 and m_2. Although the resulting integral can not be evaluated exactly, different approximations can be found, as will be discussed in the next subsections.

3.1. Approximation I

The first approximation we describe makes use of the stationary phase approximation. If ${\rm d}\psi/{\rm d}f = 0$ at a frequency $f_{\rm s}$, we can approximate $\psi(f)$ around $f_{\rm s}$ with a second order power series,

$$\psi(f) \approx \psi(f_{\rm s}) + \beta(f - f_{\rm s})^2. \tag{9}$$

For the Newtonian chirp this holds and we have

$$f_{\rm s} = \left(\frac{5}{256\pi}\right)^{3/8} \zeta^{-5/8} t^{-3/8} = f_0 \left(\frac{\tau_0}{t}\right)^{3/8} \tag{10}$$

$$\beta = \frac{5}{96} f_{\rm s}^{-11/3} \zeta^{-5/3} \tag{11}$$

where τ_0 is the first *chirp time* evaluated using f_0 as the fiducial frequency [12]. Note that $f_{\rm s}$ is a function of time and we are evaluating a family of integrals parametrized by t. The factor $f^{-7/6} S_{\rm n}^{-1}(f)$ in (7) varies more slowly with frequency than the exponential, so we take it as constant and evaluate it at $f_{\rm s}$. The integrand can then be rewritten as

the product of two Gaussians, one real and one complex, so the matched filter output is (omitting irrelevant phase factors)

$$z(t) \approx 2\sqrt{\pi}\tau \frac{f_{\rm s}^{-7/6}}{S_{\rm n}(f_{\rm s})} \int_{f_{\rm L}}^{f_{\rm H}} \exp\left(i\frac{(f-f_{\rm s})^2}{2\sigma_{\rm f}^2} - \frac{(f-f_0)^2}{2\sigma_{\rm sg}^2} \right) {\rm d}f \tag{12}$$

where $\sigma_{\rm sg} = 1/\sqrt{2}\pi\tau$ and $\sigma_{\rm f} = \sqrt{3f_0/16\pi\tau_0}(f_{\rm s}/f_0)^{11/6}$ are the standard deviations of the Gaussians. Using (12) and (3) in (1), and carrying out the integral using Cauchy's theorem, we get

$$\rho(t) \approx \frac{1}{\sigma_0} \frac{\exp\left(-\frac{(f_0-f_{\rm s})^2}{2\sigma_{\rm f}^2} \frac{\sigma_{\rm sg}^2/\sigma_{\rm f}^2}{1+\sigma_{\rm sg}^4/\sigma_{\rm f}^4} \right)}{f_{\rm s}^{7/6} S_{\rm n}(f_{\rm s})(1+\sigma_{\rm sg}^4/\sigma_{\rm f}^4)^{1/4}} \tag{13}$$

with $\sigma_0^2 = \int_0^\infty f^{-7/3} S_{\rm n}^{-1}(f) {\rm d}f$.

This is a complicated function of t through $f_{\rm s}$ and $\sigma_{\rm f}$. In particular note that t also enters via $S_{\rm n}(f_{\rm s})$ and so the shape of the SNR pulse depends on the PSD of the noise. Although $S_{\rm n}(f)$ can in principle be modeled as a combination of power laws, the resulting expression is complicated and a numerical maximization is thus needed in order to determine $\hat{\rho}$ and $\hat{t}$.

3.2. Approximation II

Our second method is a slightly different application of the stationary phase approximation and is expected to be appropriate for small Q. In fact, we still use (9) but we now assume that the largest contribution to the integral in (7) comes from a narrow band around $f_{\rm s}$. Within this band, we can thus consider all other terms of the integrand constant and equal to their value at $f_{\rm s}$, including the sine-Gaussian peak, so the integral reduces to

$$\int_{f_{\rm L}}^{f_{\rm H}} e^{i\beta(f-f_{\rm s})^2} {\rm d}f \approx \sqrt{\frac{\pi}{\beta}}. \tag{14}$$

Therefore, omitting all irrelevant phase terms,

$$z(t) \approx 2\pi\tau h_0 \frac{\exp\left(-\pi^2\tau^2(f_{\rm s}-f_0)^2\right)}{f_{\rm s}^{7/6} S_{\rm n}(f_{\rm s})\beta^{1/2}} \tag{15}$$

and the resulting SNR time series is

$$\rho(t) \approx \frac{\pi\tau}{\sigma_0} \frac{\exp\left(-\pi^2\tau^2(f_{\rm s}-f_0)^2\right)}{f_{\rm s}^{7/6} S_{\rm n}(f_{\rm s})\beta^{1/2}}. \tag{16}$$

For the Newtonian chirp,

$$\rho(t) \approx \frac{\sqrt{6}\pi^{3/4}}{5^{1/4}} \frac{\tau\zeta^{5/12}}{\sigma_0} \frac{\exp\left(-\pi^2\tau^2(f_{\rm s}-f_0)^2\right)}{S_{\rm n}(f_{\rm s})} t^{-1/4}. \tag{17}$$

This is still a quite complicated function of time and it still depends on the PSD of the noise. In general, at least for a smooth PSD with no peaks, it is the product of two peaks with different time scales, one corresponding to the exponential term and the other associated with the $f_{\rm s}^{7/6} S_{\rm n}(f_{\rm s})\beta^{1/2}$ term. Thus $\hat{t}$ depends on f_0, τ, ζ and

the details of $S_{\rm n}(f)$ even for the Newtonian chirp. Although we expect approximation II to be valid for small Q, we can try to take the result to the limit of $Q \to \infty$. The exponential becomes more peaked than the $f_{\rm s}^{-7/6} S_{\rm n}^{-1}(f_{\rm s})\beta^{-1/2}$ term, so $\rho(t)$ is maximum where $f_{\rm s} = f_0$ and

$$\hat{\rho} \approx \frac{\pi\tau}{\sigma_0} f_0^{-7/6} S_{\rm n}^{-1}(f_0)\beta^{-1/2} \tag{18}$$

$$\hat{t} \approx \tau_0. \tag{19}$$

This suggests that in the large Q limit the trigger delay is just the time the inspiral takes to coalesce after crossing the center frequency of the sine-Gaussian, which can be expected from intuition. As we said, however, this approximation is expected to work for small Q and thus in general $\hat{\rho}$ and $\hat{t}$ must be found numerically.

3.3. Approximation III

Although probably less useful in practice, a different approximation can be derived in the large Q limit. In this regime the integrand in (7) is no longer dominated by the band around $f_{\rm s}$ but by the narrow peak of the sine-Gaussian, centered on f_0. Again, the factor $f^{-7/6} S_{\rm n}^{-1}(f)$ varies slowly with frequency and can be regarded as constant, and the integral limits can be extended over the real axis. We still approximate the template phase as a second-order Taylor series, but this time around f_0,

$$\psi(f) \approx \psi(f_0) + \alpha(f - f_0) + \beta(f - f_0)^2. \tag{20}$$

For instance, for the Newtonian chirp we have

$$\alpha = 2\pi t - \frac{5}{128} f_0^{-8/3} \zeta^{-5/3} = 2\pi(t - \tau_0) \tag{21}$$

$$\beta = \frac{5}{96} f_0^{-11/3} \zeta^{-5/3}. \tag{22}$$

After switching the integration variable to $x = \sqrt{\pi^2\tau^2 - i\beta}(f - f_0)$, and omitting irrelevant phase factors, we are left with a Gaussian integral

$$z(t) \approx \frac{2\sqrt{\pi}\tau h_0}{\sqrt{\pi^2\tau^2 - i\beta}} \frac{f_0^{-7/6}}{S_{\rm n}(f_0)} \int_{-\infty}^{+\infty} \exp\left(-x^2 + \frac{i\alpha x}{\sqrt{\pi^2\tau^2 - i\beta}}\right) {\rm d}x \tag{23}$$

which readily gives

$$z(t) \approx \frac{2\pi\tau h_0}{\sqrt{\pi^2\tau^2 - i\beta}} \frac{f_0^{-7/6}}{S_{\rm n}(f_0)} \exp\left(-\frac{\alpha^2}{4(\pi^2\tau^2 - i\beta)}\right). \tag{24}$$

The final expression for the approximated SNR time series is

$$\rho(t) \approx \frac{1}{\sigma_0} \frac{\exp\left(-\alpha^2/4\pi^2\tau^2(1 + \frac{\beta^2}{\pi^4\tau^4})\right)}{f_0^{7/6} S_{\rm n}(f_0) \left(1 + \frac{\beta^2}{\pi^4\tau^4}\right)^{1/4}}. \tag{25}$$

In the case of the Newtonian chirp α is the only function of time, so $\rho(t)$ is a simple Gaussian pulse and we obtain explicit expressions for trigger SNR and time,

$$\hat{\rho} \approx \sigma_0^{-1} f_0^{-7/6} S_{\rm n}^{-1}(f_0) \left(1 + \frac{\beta^2}{\pi^4\tau^4}\right)^{-1/4} \tag{26}$$

$$\hat{t} \approx \tau_0. \tag{27}$$

Note that $\hat{t}$ is consistent with approximation II taken in the limit of large Q, but $\hat{\rho}$ is not and we expect approximation III to give the correct result in this case.

4. Numerical simulations

We test the accuracy of the approximations by numerically computing the response of an inspiral matched filter to noiseless sine-Gaussians injected in the time domain. For $S_{\rm n}(f)$ we take the noise PSD corresponding to advanced LIGO's *zero detuning, high power* configuration, an approximation of which is provided by the LALSimulation module of LALSuite [13]. For simplicity, and in order to work well within the numerical range of the floating-point representation, we set the amplitude of the simulated sine-Gaussian to 1 and at the same time we scale the noise PSD by 10^{48}; therefore, the resulting trigger SNR refers to sine-Gaussians with an amplitude of $A = 10^{-24}$. We scan the (f_0, Q) parameter space in the region 10 Hz $\leq f_0 \leq \min(1\ \text{kHz}, f_{\rm ISCO})$, $1 \leq Q \leq 1000$ for total mass values of $2.8M_\odot$, $5M_\odot$ and $10M_\odot$. For each point, we compute the maximum SNR $\hat{\rho}$ and the delay $\hat{t}$ between the maximum SNR and the center of the injected sine-Gaussian, and we compare to the predicted values. Results for approximation I, II and III can be seen in figure 1, 2 and 3 respectively.

Approximation I works well for both $\hat{\rho}$ and $\hat{t}$, but it degrades for large values of f_0, Q or mass. In particular, we find that surfaces of constant accuracy roughly match those of constant $f_0^2 QM$; the 5% accuracy for SNR, at least in the explored parameter range, is at $f_0^2 QM/M_\odot \approx 5 \times 10^7\ \text{s}^{-2}$. This is likely not a major problem, as we expect most glitches to last at most tens of cycles and affect mostly low frequencies. Moreover, at high frequency or mass the time delay is small and thus the problem we are considering is less important. Also note that neglecting the second exponential of (6) produces no noticeable effects even for $Q \approx 1$.

Approximation II produces excellent estimates of the time delay across all the explored parameter space, but wrong estimates of SNR for large Q, as can be expected. In fact, as Q increases, the sine-Gaussian peak in the frequency domain shrinks and at some point the integral is no longer dominated by the region around $f_{\rm s}$. Since we are interested in the low-Q region, despite this problem this is still a useful approximation, although not significantly simpler than I.

As expected, approximation III works very well in the high mass, high Q region where the other two approximations do not give such good results. Moreover it is analytically simpler. But for a large region of the parameter space where Q is small, this approximation fails and so is not so useful for a large part of the parameter space of interest. This is because the width of the Gaussian in the frequency domain becomes comparable or larger than the width of the other terms in the integrand and the approximation is not valid. However, in this part of the parameter space we can simply revert to approximations I and II.

Although our calculations are based on the Newtonian chirp, search pipelines use inspiral waveforms with higher post-Newtonian order [6]. Thus we also check the

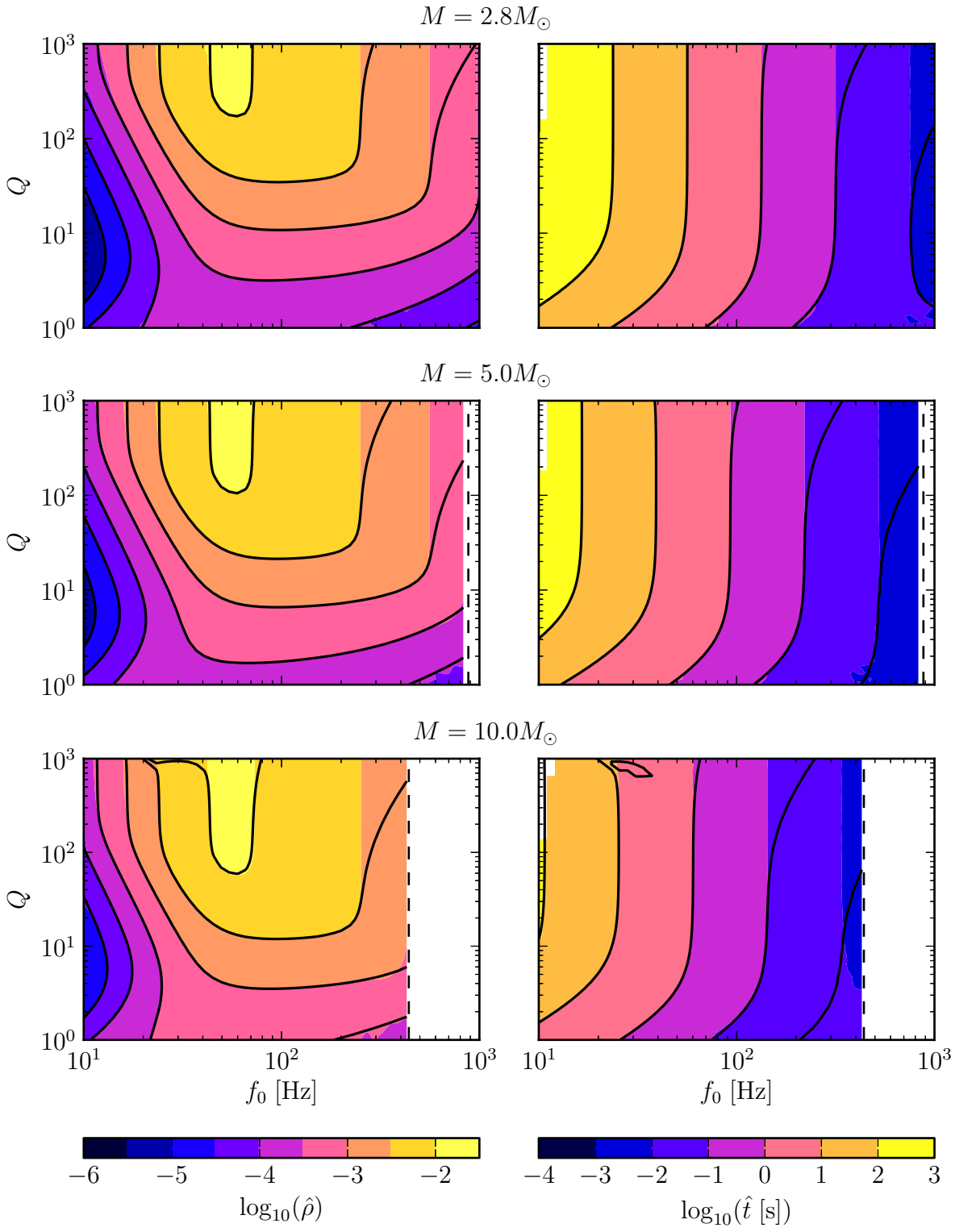

Figure 1. Comparison between simulations (shaded bands, color online) and approximation I (black contours) for different total masses. Left plots show the trigger SNR, right ones the delay. The dashed line is the ISCO frequency. As can be seen, this approximation fails for large f_0, Q or M.

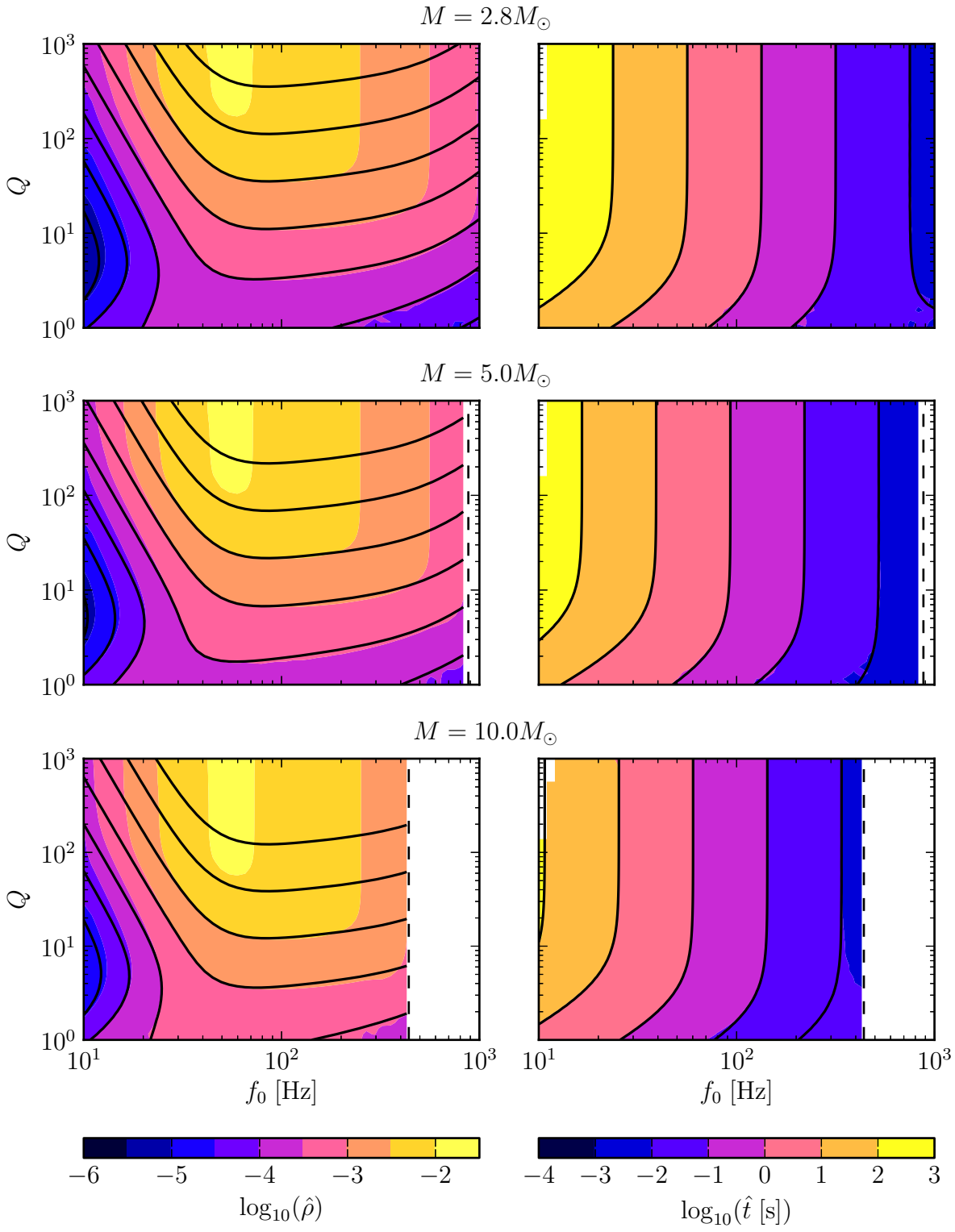

Figure 2. Comparison between simulations (shaded bands, color online) and approximation II (black contours) for different total masses. Left plots show the trigger SNR, right ones the delay. The dashed line is the ISCO frequency. The SNR predicted by approximation II is not correct for $Q \gg 1$, as expected. Remarkably however, the predicted trigger time is good for most of the explored parameter space.

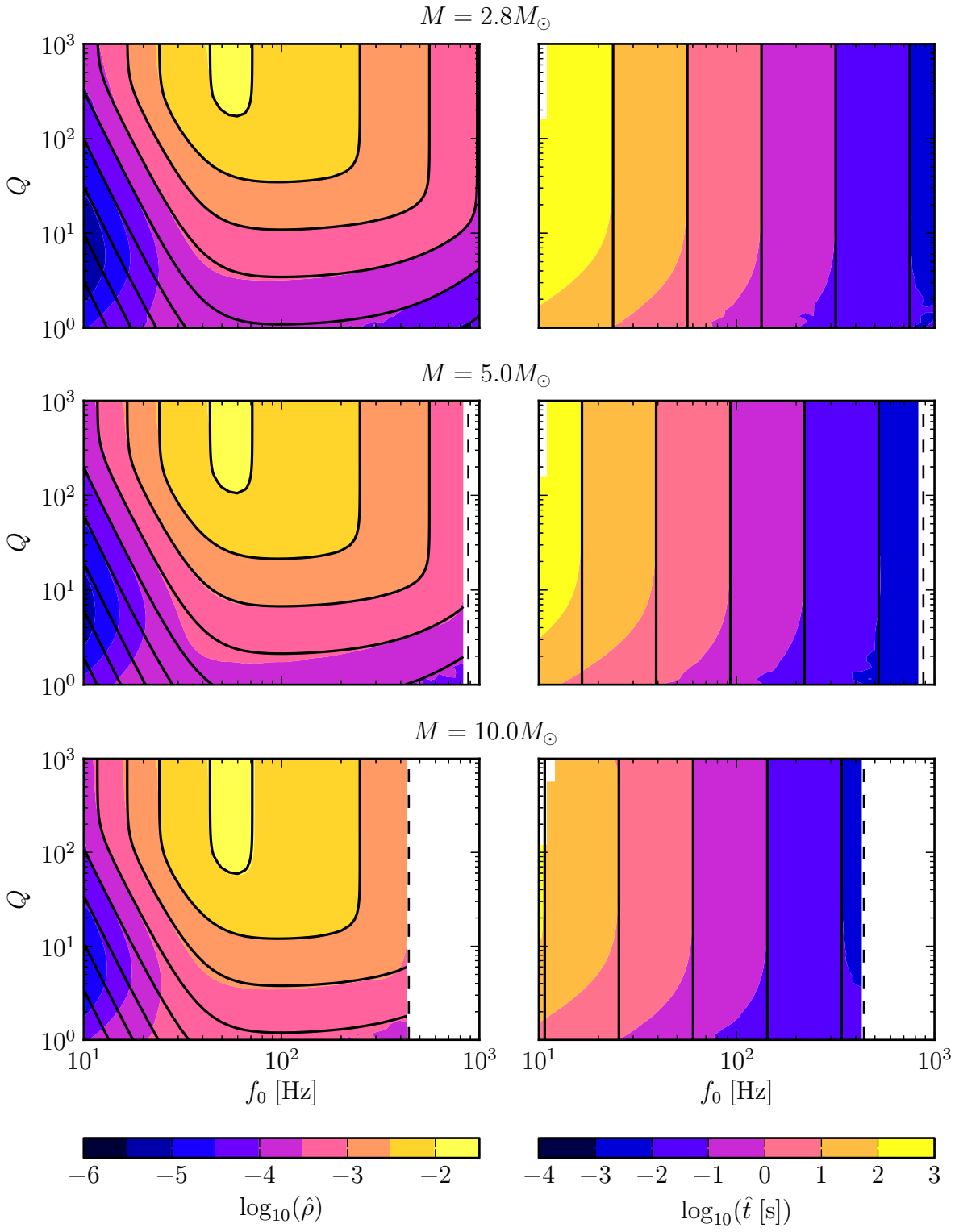

Figure 3. Comparison between simulations (shaded bands, color online) and approximation III (black contours) for different total masses. Left plots show the trigger SNR, right ones the delay. The dashed line is the ISCO frequency. As expected, approximation III does not work for small Q.

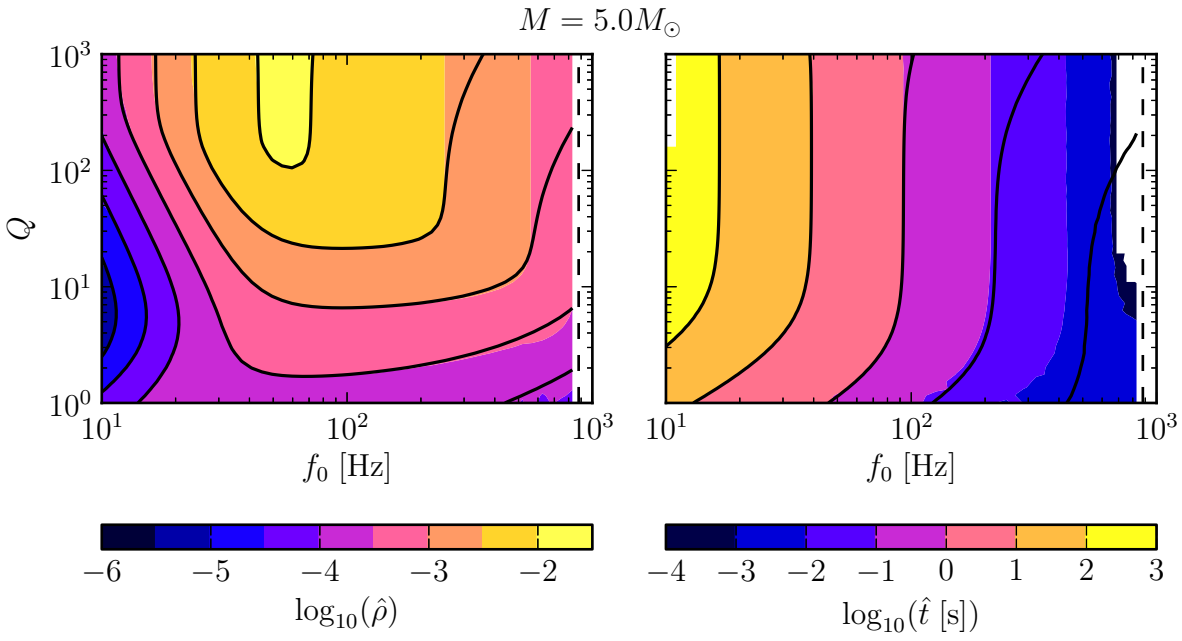

Figure 4. Comparison between a simulation using a 3.5PN equal-mass inspiral waveform (shaded bands, color online) and approximation I (black contours) for a total mass of $5M_\odot$. The left plot is the trigger SNR, the right one is the trigger delay. The dashed line is the ISCO frequency.

accuracy of the approximations against simulations using a 3.5PN inspiral filter. We find that the accuracy degrades but is still within a few percent both for $\hat{\rho}$ and $\hat{t}$ and it retains a similar dependency on f_0, Q and M. An example for a $5M_\odot$ equal-mass binary is shown in figure 4. Since our approximations are based simply on power-series approximations of the inspiral phase, they can in principle accommodate high post-Newtonian order waveforms, at the price of more complicated expressions for $\rho(t)$.

In a search pipeline, the parameter space of the binary is covered by a template bank. A true inspiral signal produces triggers only for templates whose parameters are close enough to the true values, depending on the ambiguity function of the waveform. However, a strong glitch generally excites a significant fraction of the whole bank, producing a cluster of triggers with different SNRs and times. An example of this phenomenon is shown in figure 5, where we plot the distribution of triggers in $(\hat{t}, \hat{\rho})$ corresponding to a sine-Gaussian glitch affecting a simplified template bank with uniform distribution in total mass. The dependency of SNR and time delay on the template mass determines the shape of the cluster. Low-mass templates produce the triggers with the largest delay and smallest SNR. The last triggers can be delayed by several minutes, which is much longer than the duration of the glitch (typically seconds or fractions of a second).

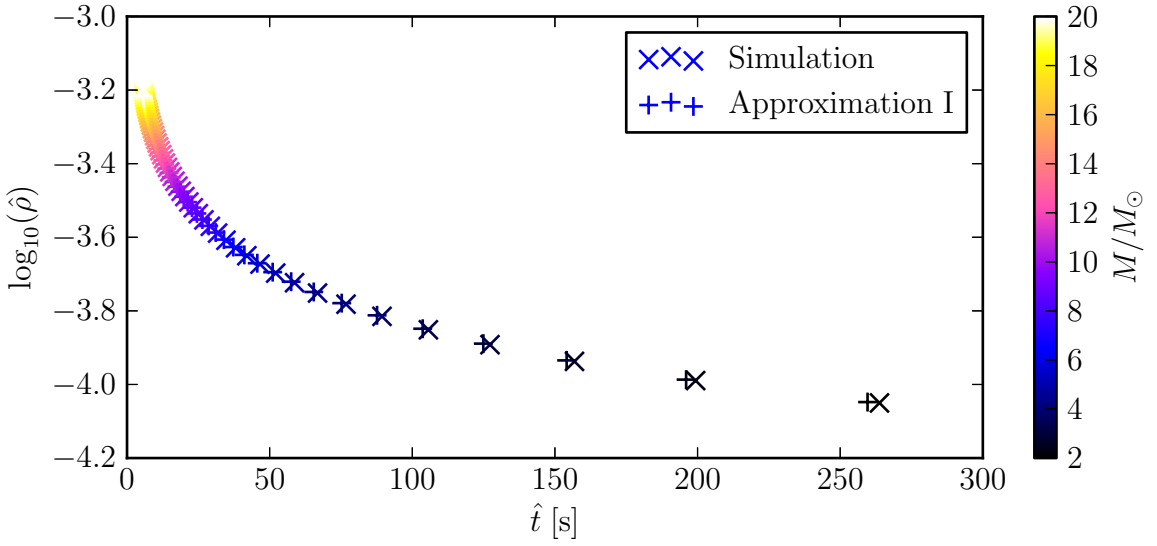

Figure 5. Cluster of triggers generated by a template bank responding to a sine-Gaussian glitch with $t_0 = 0$, $f_0 = 20$ Hz and $Q = 20$. The bank consists of 50 3.5PN, equal-mass waveforms with M uniformly spaced in $[2M_\odot, 20M_\odot]$. The cluster extends well after the duration of the glitch, with the lowest mass templates still producing triggers minutes after the glitch.

5. Conclusion

Low-mass waveforms represent a potential problem for future inspiral searches and in particular for low-latency BNS pipelines such as MBTA [14] and LLOID [15]. In fact, as evident from this study, low-mass triggers generated by glitches could be delayed by several minutes. The result is that a single glitch could produce a cluster of many spurious triggers lasting for several minutes. Although we found that the trigger SNR effectively decreases with increasing delay, glitches can be very strong and still produce triggers with a large delay and SNR above the detection threshold. Consistency tests such as the χ^2 test [16] and its variations [17] are most effective for long waveforms and would likely rule out a large fraction of such spurious triggers. Indeed, a detailed investigation of the response of these tests is a possible followup of this work. Unfortunately however, the efficiency of such tests also decreases with decreasing SNR. Triggers with large delay and SNR just above the detection threshold will therefore still be problematic and veto procedures based on auxiliary channels will be important.

We presented three approximations which allow one to predict the SNR and time of triggers generated by an inspiral matched filter responding to sine-Gaussian glitches. We compared them to numerical simulations and investigated their validity in the region of (f_0, Q, M) parameter space relevant for advanced detectors. Together they complement each other, providing full coverage of the explored region. They could be useful for determining whether an inspiral trigger can be associated with an excitation of auxiliary channels. In fact, the knowledge of the trigger SNR and mass could be used to

determine a possible set of (t_0, f_0, Q) parameters and test the hypothesis that the trigger was produced by a sine-Gaussian glitch with such parameters in an auxiliary channel. Note that sine-Gaussians are the signal basis used by the Omega pipeline [18]—a tool widely used by the LIGO collaboration for data quality assessment—and therefore the integration of our results into this tool is straightforward. Another possible application is searching for clusters of triggers across the template bank whose distribution in SNR and time matches the one predicted by the approximations. This could provide a way of simultaneously vetoing all triggers belonging to such clusters. The definition of procedures for actively exploiting our approximations is another natural followup of this paper.

Acknowledgments

We thank Tom Dent, Drew Keppel, Badri Krishnan and Alex Nielsen for useful discussion and comments. TDC is supported by the IMPRS on Gravitational Wave Astronomy. SVD and SB would like to thank Badri Krishnan and Bruce Allen for supporting their visits to AEI, Hannover, Germany. SVD would like to thank IUCAA, Pune, India for a visiting professorship where this work was completed. This paper has LIGO document number LIGO-P1300016.

References

[1] Harry G M et al. 2010 Advanced LIGO: the next generation of gravitational wave detectors *Class. Quant. Grav.* **27** 084006
[2] Acernese F et al. 2009 Advanced Virgo Baseline Design *Virgo Technical Report* VIR-0027A-09
[3] Abadie J et al. 2010 Predictions for the Rates of Compact Binary Coalescences Observable by Ground-based Gravitational-wave Detectors *Class. Quant. Grav.* **27** 173001
[4] Blanchet L 2006 Gravitational Radiation from Post-Newtonian Sources and Inspiralling Compact Binaries *Living Rev. Rel.* **9**
[5] Babak S et al. 2012 Searching for gravitational waves from binary coalescence (*preprint* arXiv:1208.3491 [gr-qc])
[6] Allen B et al. 2012 FINDCHIRP: an algorithm for detection of gravitational waves from inspiraling compact binaries *Phys. Rev. D* **85** 122006
[7] Blackburn L et al. 2008 The LSC Glitch Group: Monitoring Noise Transients during the fifth LIGO Science Run *Class. Quant. Grav.* **25** 184004
[8] Slutsky J et al. 2010 Methods for reducing false alarms in searches for compact binary coalescences in LIGO data *Class. Quant. Grav.* **27** 165023
[9] Aasi J et al. 2012 The characterization of Virgo data and its impact on gravitational-wave searches *Class. Quant. Grav.* **29** 155002
[10] Sathyaprakash B S and Dhurandhar S V 1991 Choice of filters for the detection of gravitational waves from coalescing binaries *Phys. Rev. D* **44** 3819
[11] Peters P C and Mathews J 1963 Gravitational Radiation from Point Masses in a Keplerian Orbit *Phys. Rev.* **131** 435-440
[12] Sengupta A S et al. 2003 A faster implementation of the hierarchical search algorithm for detection of gravitational waves from inspiraling compact binaries *Phys. Rev. D* **67** 082004
[13] https://www.lsc-group.phys.uwm.edu/daswg/projects/lalsuite.html

[14] Beauville F et al. 2008 Detailed comparison of LIGO and Virgo Inspiral Pipelines in Preparation for a Joint Search *Class. Quant. Grav.* **25** 045001

[15] Cannon K et al. 2012 Toward Early-warning Detection of Gravitational Waves from Compact Binary Coalescence *ApJ* **748** 136

[16] Allen B 2005 A chi-squared time-frequency discriminator for gravitational wave detection *Phys. Rev. D* **71** 062001

[17] Hanna C 2008 Searching for gravitational waves from binary systems in non-stationary data *PhD thesis, Louisiana State University*

[18] Chatterji, S K 2005 The search for gravitational wave bursts in data from the second LIGO science run *PhD thesis, MIT Dept. of Physics*